

## Improvement of tip analysis model for drilled shafts in cohesionless soils

Yit-Jin Chen <sup>\*1</sup>, Hao-Wei Wu <sup>1a</sup>, Maria Cecilia M. Marcos <sup>1,2b</sup> and Shiu-Shin Lin <sup>1c</sup>

<sup>1</sup> Department of Civil Engineering, Chung Yuan Christian University, Chung-Li, 32023, Taiwan

<sup>2</sup> Department of Civil Engineering, Adamson University, Manila, Philippines

(Received September 24, 2012, Revised April 10, 2013, Accepted May 18, 2013)

**Abstract.** An analysis model for predicting the tip bearing capacity of drilled shafts in cohesionless soils is improved in this study. The evaluation is based on large amounts of drilled shaft load test data. Assessment on the analysis model reveals a greater variation in two coefficients, namely, the overburden bearing capacity factor ( $N_q$ ) and the bearing capacity modifier for soil rigidity ( $\zeta_{qr}$ ). These factors are modified from the back analysis of drilled shaft load test results. Different effective shaft depths and interpreted capacities at various loading stages (i.e., low, middle, and high) are adopted for the back calculation. Results show that the modified bearing capacity coefficients maintain their basic relationship with soil effective friction angle ( $\bar{\phi}$ ), in which the  $N_q$  increases and  $\zeta_{qr}$  decreases as  $\bar{\phi}$  increases. The suggested effective shaft depth is limited to 15B (B = shaft diameter) for the evaluation of effective overburden pressure. Specific design recommendations for the tip bearing capacity analysis of drilled shafts in cohesionless soils are given for engineering practice.

**Keywords:** drilled shafts; cohesionless soils; tip bearing capacity; friction angle; effective shaft depth

### 1. Introduction

Tip resistance is an essential source of drilled shaft capacity under axial compression loading. The contribution of tip resistance is relatively significant for shorter shafts or when the shaft penetrates through layers of soft soils where side resistance is limited. Various soil-bearing capacity equations from the literature can be applied to estimate the tip capacity.

Researchers (Hansen 1970, Vesic 1975, Kulhawy *et al.* 1983) have continually improved the general solution of the ultimate soil bearing capacity ( $q_{ult}$ ). Often, to evaluate the ability of an analysis model to predict shaft capacity, field load tests are used (Zhang *et al.* 2006, Schneider *et al.* 2008, Cai *et al.* 2009, 2012, Ching and Chen 2010) because they provide a convenient way of comparison between predicted and measured capacities. Recently, Chen *et al.* (2009), based on a wide range of compression field load test data, performed an extensive evaluation of tip bearing capacity of drilled shafts from a representative analysis model. The examined model (Kulhawy

\*Corresponding author, Professor, E-mail: [yjc@cycu.edu.tw](mailto:yjc@cycu.edu.tw)

<sup>a</sup> Master Science

<sup>b</sup> Ph.D. Student, Instructor, E-mail: [g9802203@cycu.edu.tw](mailto:g9802203@cycu.edu.tw)

<sup>c</sup> Associate Professor, E-mail: [linxx@cycu.edu.tw](mailto:linxx@cycu.edu.tw)

1991) was a modified Terzaghi-Buisman equation for the solution of  $q_{ult}$  (Vesic 1975). Although such prediction method provided reasonable results for shafts in cohesive soils, this method greatly overestimated the tip capacity of drilled shafts in cohesionless soils as shown in Fig. 1. On the average, the predicted result is approximately 9-times higher than the measured result. The same model was also adopted in the studies by Chen (2010) and Marcos *et al.* (2011) for pre-bored precast concrete piles and by Chu (2009) for drilled shafts in gravelly soils. Results from these studies show similar tip capacity overprediction with varying degrees, which can be attributed to the differences in pile construction and installation.

Chen *et al.* (2009) further analyzed possible reasons that caused overestimation in cohesionless soils. According to their previous findings, overestimation is most likely caused by the effective overburden pressure ( $\bar{q}$ ), overburden bearing capacity factor ( $N_q$ ), and other related analysis coefficients. Improvement of these factors had been suggested. Vesic (1963) and the Department of the Navy, Naval Facilities Engineering Command (1982) also focused on the study of bearing capacity and explained that the point bearing capacity of a pile in sandy soils generally increases with depth, up to a so-called critical depth. The capacity becomes constant beyond this depth. Hence, for relatively large pile lengths, the analysis of effective overburden pressure can reach a maximum value at a depth of embedment known as the effective depth.

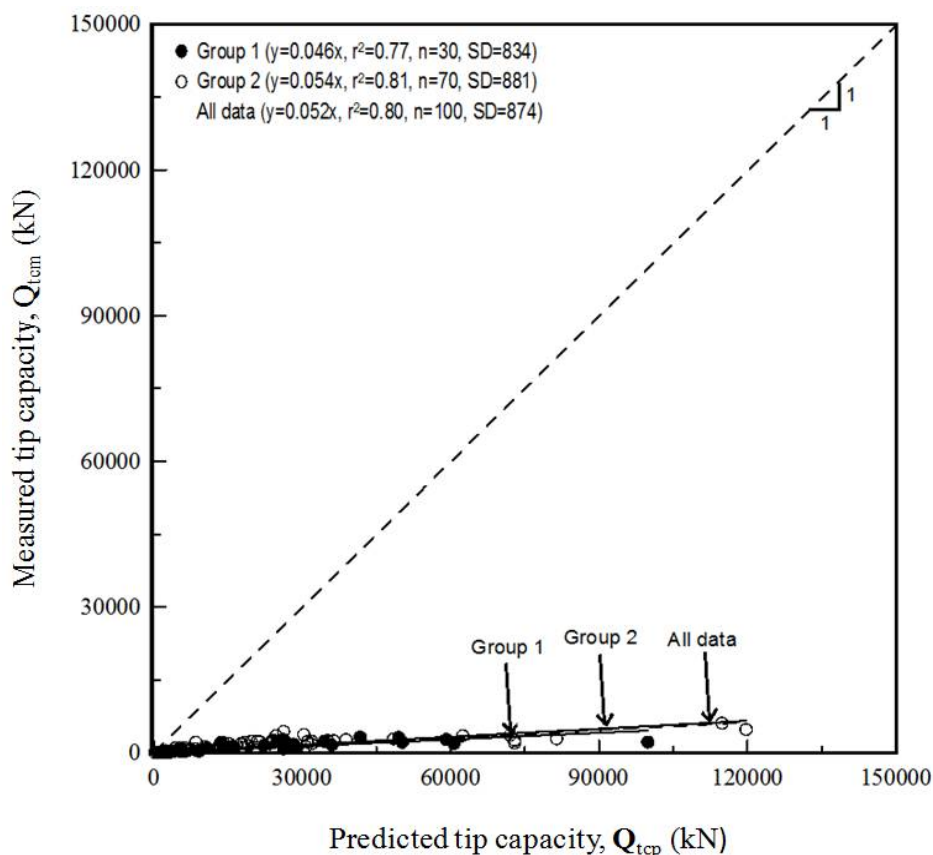


Fig. 1 Comparison of predicted and measured tip resistances in cohesionless soils (Chen *et al.* 2009)

In the present study, an analysis model for calculating the tip bearing capacity is carefully improved to predict more efficiently the behavior of drilled shafts in cohesionless soils. The modification is based on back-analysis utilizing a large number of drilled shaft field load test data. The authors, however, are aware that the improvement can be fully accomplished in the light of theory. Nevertheless, this study can practically be adopted for preliminary drilled shaft design or practical engineering application. Information on drilled shaft load tests is collected for the evaluation. The variability of each factor in the analysis model is first determined, and the factors that exhibit great variation are critically assessed and modified.

## 2. Drilled shaft load test data

The current study primarily aims to extend the research of Fang (2007) and Chen *et al.* (2009), specifically on the cohesionless soil analysis for drilled shafts. The aforementioned researchers collected 100 compression field load tests in 56 sites for cohesionless soils. All of the selected tests had almost complete geological data and load-displacement curves, and all were conducted on straight-sided drilled shafts. The basic information and interpreted capacities of these shafts are shown in Table 1. Both the total and tip interpreted capacities that were deduced from selected interpretation criteria are indicated in the table. All of the data were from field test information and load-displacement results of static shaft load tests. The amount of data is sufficiently large, reflecting common field situations, and the data can be a representative for the evaluation. The construction method is listed to assess the influence of shaft installation procedures on tip capacity. Based on the available data in Table 1 and the result in Fig. 1, the difference in behavior of various construction methods is minimal.

The interpretation criteria  $L_1$ - $L_2$  by Hirany and Kulhawy (1988, 2002) and Chin method (Chin 1970) were selected to measure the load carrying capacity of the shafts. The  $L_1$ - $L_2$  is a graphical construction method, where  $L_1$  is defined as the load at the end of the initial region of the load-displacement curve (elastic limit), and  $L_2$  is the load at the initiation of the final linear region

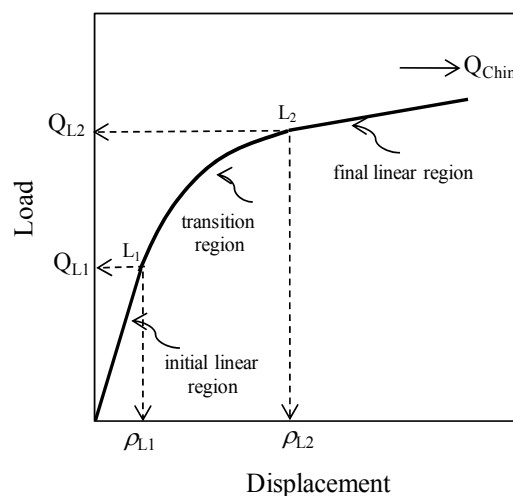


Fig. 2 Regions of  $L_1$ ,  $L_2$ , and Chin interpretation criteria within the load-displacement curve

Table 1 Load test data for drilled shafts in cohesionless soils (Fang 2007)

Pile No.	Location/Soil description	Depth, D(m)	Dia., B(m)	$\gamma_m^a$ (kN/m <sup>3</sup> )	GWT <sup>b</sup> (m)	$\bar{q}^c$ (kN/m <sup>2</sup> )	$\bar{\phi}^d$ (°)	Const. method <sup>m</sup>	$Q_{top}^e$	$Q_{L1}^f$	$Q_{L2}^g$	$Q_{Chin}^h$	$Q_{L1(tp)}^i$	$Q_{L2(tp)}^j$	$Q_{Chin(tp)}^k$
1	Roorkee, India/sand	5.5	0.64	15.5	0.6	37	31	dry	561	298	685	934	33	137	386
2	Galveston, Texas/silty sand	18.0	1.20	19.6	0.0	177	32	-	5195	1872	4250	6258	206	523	2857
3	Galveston, Texas/silty sand	20.0	0.91	19.6	6.1	256	32	-	3600	923	2147	3506	102	429	1788
4	Galveston, Texas/silty sand	18.0	0.91	19.6	6.1	236	33	-	3670	1379	3529	4967	152	658	2144
5	Ontario, Canada/loose silt with sand & clay	6.4	1.07	19.6	1.0	73	33	slurry	173	96	180	253	11	36	109
6	Laboratory test/sand	5.0	0.24	20.0	5.0	100	33	casing	2848	378	1601	3274	42	305	1994
7	Taichung, Taiwan/silty sand	60.0	1.20	19.6	2.0	608	34	-	11304	2395	5560	9063	263	1112	4615
8	Taichung, Taiwan/silty sand	60.0	1.50	19.6	2.0	608	34	-	17758	5420	12615	18487	596	2523	8395
9	Taichung, Taiwan/silty sand	60.0	2.00	19.6	2.0	608	34	-	31661	7570	17605	28696	833	3521	14612
10	Chiayi, Taiwan/silty fine sand	34.7	1.50	19.6	1.0	350	34	-	14049	6227	10675	17400	685	2415	8860
11	Chiayi, Taiwan/silty fine sand	34.7	1.50	19.6	1.0	350	34	-	14138	6939	10675	16040	763	830	7500
12	Chiayi, Taiwan/silty fine sand	34.7	1.50	19.6	1.0	350	34	-	14160	6109	11236	15783	672	2723	6795
13	Sao Paulo, Brazil/clayey sand	10.0	0.35	19.6	- <sup>l</sup>	196	34	dry	569	146	300	489	16	107	249
14	Sao Paulo, Brazil/clayey sand	10.0	0.40	19.6	- <sup>l</sup>	196	35	dry	760	211	448	730	23	162	372
15	Sao Paulo, Brazil/clayey sand	10.0	0.50	19.6	- <sup>l</sup>	196	35	dry	1188	220	386	806	24	204	498
16	Crystal River, Florida/sand over limestone	8.2	0.48	17.3	1.1	72	35	-	660	285	610	994	31	122	506
17	Wuhan, China/medium dense silty fine sand	12.0	0.76	19.6	0.0	118	35	-	2131	1400	2470	3400	154	220	1424
18	Wuhan, China/medium dense silty fine sand	12.0	0.76	19.6	0.0	118	35	-	2136	1200	2040	3325	132	360	1693
19	Wuhan, China/medium dense silty fine sand	12.0	0.76	19.6	0.0	118	35	-	2141	800	1500	2472	88	280	1272
20	Kaohsiung, Taiwan/loose fine sand	15.0	1.20	19.6	0.0	147	35	casing	6066	1220	2600	5292	134	588	3212
21	Houston, Texas/sand	14.3	0.76	19.6	7.0	209	35	-	3072	2131	4196	6572	234	1085	3215
22	Houston, Texas/sand	18.6	0.92	19.6	7.0	251	35	-	4949	2293	4209	6861	252	439	3493
23	Kaohsiung, Taiwan/fine sand	52.5	1.20	19.6	1.0	525	36	casing	12096	6100	12378	16867	671	2476	6964
24	Taipei, Taiwan/fine silty sand	39.0	1.20	19.6	1.0	392	36	slurry	10872	5150	11765	16135	567	2353	6723
25	Sao Paulo, Brazil/loose fine silty sand	19.3	1.20	17.3	4.7	147	36	-	6947	2280	5000	8100	251	1000	4100

Pile No.	Location/Soil description	Depth, D(m)	Dia., B(m)	$\gamma_m^a$ (kN/m <sup>3</sup> )	GWT <sup>b</sup> (m)	$\bar{q}^c$ (kN/m <sup>2</sup> )	$\bar{\phi}^d$ (°)	Const. method <sup>m</sup>	$Q_{tip}^e$	$Q_{L1}^f$	$Q_{L2}^g$	$Q_{Chin}^h$	$Q_{L1(ip)}^i$	$Q_{L2(ip)}^j$	$Q_{Chin(ip)}^k$
(kN)															
26	Texas/cemented clayey sand	4.7	0.93	19.6	0.3	92	36	- <sup>n</sup>	3168	2669	5338	10086	294	1041	5816
27	Sao Paulo, Brazil/loose fine silty sand	34.0	1.50	19.6	1.0	343	37	casing	16737	8150	18885	26733	897	3777	11625
28	Glasgow, U.K./silty fine & medium sand	17.5	0.50	17.8	6.0	199	37	- <sup>n</sup>	1427	1160	2483	3288	128	407	1302
29	JFK Airport, New York/sand	18.3	0.92	18.1	1.5	166	37	- <sup>n</sup>	4433	1495	3444	5614	164	689	2859
30	Yellow River Bridge, China/silt & fine sand	62.0	1.10	18.1	0.0	514	37	- <sup>n</sup>	11208	5620	11563	15289	618	2313	6039
31	Walkerton, Ontario/sand over clayey silt	6.4	1.07	21.0	0.6	78	37	slurry	4328	860	2000	3260	95	400	1660
32	Honshu-Shikoku, Japan/sand	68.5	2.00	21.0	0.0	767	37	- <sup>n</sup>	47498	12940	35821	43958	1423	2219	15301
33	Tampa Bay, Florida/ loose to med fine sand	11.6	0.92	18.1	5.5	150	38	dry	4475	956	2224	3625	105	445	1846
34	Glasgow, U.K./silty fine & medium sand	17.5	0.50	17.8	6.0	199	38	- <sup>n</sup>	1533	894	2078	2821	98	313	1159
35	Glasgow, U.K./silty fine & medium sand	17.5	0.50	17.8	6.0	199	38	- <sup>n</sup>	1535	1008	2344	3145	111	379	1270
36	Glasgow, U.K./silty fine & medium sand	16.0	0.50	17.8	6.0	187	38	- <sup>n</sup>	1491	756	1759	2436	83	297	1028
37	Glasgow, U.K./silty fine & medium sand	20.0	0.50	17.8	6.0	219	38	- <sup>n</sup>	1613	1126	2618	3480	124	338	1386
38	Tainan, Taiwan/loose sand	30.2	1.20	19.6	0.5	301	38	- <sup>n</sup>	8943	3035	7598	9884	334	1520	3806
39	Bangkok, Thailand/dense to very dense sand	54.0	1.50	21.0	1.0	614	38	slurry	24230	6199	14395	23464	682	2879	11948
40	Tainan, Taiwan/silty sand	25.0	1.20	19.6	1.0	255	38	dry	10279	2621	5137	8373	288	1135	4263
41	Tampa Bay, Florida/ clayey sand	12.8	0.92	17.6	4.9	148	38	dry	4762	1890	4003	6525	208	801	3322
42	NR/loose to medium sand	5.5	0.64	17.3	- <sup>l</sup>	95	39	dry	1871	245	533	872	27	107	445
43	Japan/sand	9.4	1.00	18.9	0.5	90	39	- <sup>n</sup>	4813	1445	3204	5223	159	641	2659
44	Bangkok, Thailand/dense to very dense sand	51.0	1.00	21.0	1.0	581	39	slurry	12007	5600	12992	17458	616	2598	7064
45	Bannosu, Japan/sand, gravel & clay	40.0	2.00	18.9	- <sup>l</sup>	756	40	- <sup>n</sup>	44300	15117	30500	45000	1663	6100	20600
46	Bangkok, Thailand/dense to very dense sand	57.0	1.50	21.0	1.0	648	40	slurry	28950	11954	23587	30452	1315	1903	11582
47	Bangkok, Thailand/dense to very dense sand	43.0	1.00	21.0	1.0	491	40	slurry	11351	5115	10497	14535	563	1618	6137
48	Bangkok, Thailand/sand	25.8	1.00	21.0	0.9	297	40	slurry	8936	2357	4571	6932	259	1345	3275
49	Tainan, Taiwan/silty sand	25.0	1.20	19.6	1.0	255	40	slurry	12083	2560	5016	8176	282	1100	4163
50	Orange County, Texas/fine to medium sand	20.6	0.46	19.6	0.0	202	40	- <sup>n</sup>	3010	725	1647	2685	80	329	1367
51	Brownsville, Texas/fine to medium sand	7.6	0.61	17.3	1.0	131	40	- <sup>n</sup>	2291	414	846	1379	46	169	702
52	Bangkok, Thailand/dense to very dense sand	24.0	0.60	20.0	7.6	254	40	slurry	1757	815	1545	2019	90	175	783

Pile No.	Location/Soil description	Depth, D(m)	Dia., B(m)	$\gamma_m^a$ (kN/m <sup>3</sup> )	GWT <sup>b</sup> (m)	$\bar{q}^c$ (kN/m <sup>2</sup> )	$\bar{\phi}^d$ (°)	Const. method <sup>m</sup>	$Q_{tip}^e$	$Q_{L1}^f$	$Q_{L2}^g$	$Q_{Chin}^h$	$Q_{L2(ip)}^i$	$Q_{Chin(ip)}^j$	$Q_{Chin(ip)}^k$
53	Bangkok, Thailand/dense to very dense sand	46.5	1.00	21.0	1.0	530	40	slurry	12256	7998	11921	19431	880	2419	9894
54	Central Taiwan/silty sand	36.5	1.47	19.6	- <sup>l</sup>	716	41	slurry	30911	4137	8655	10000	455	1489	3076
55	Tainan, Taiwan/fine sand	21.5	0.60	19.6	1.0	221	41	- <sup>n</sup>	2967	1479	2900	3925	163	580	1605
56	Tainan, Taiwan/fine sand	46.8	1.50	20.0	2.6	503	41	slurry	28706	10369	13203	21897	1141	2758	11335
57	Bangkok, Thailand/dense to very dense sand	50.0	0.80	21.0	1.0	569	41	slurry	8498	5611	10845	18577	617	2169	9901
58	Houston-Gulf Coastal/dense sand	18.9	0.46	19.6	1.4	199	42	slurry	1787	669	1840	2637	74	111	1165
59	Bangkok, Thailand/dense to very dense sand	26.0	0.60	20.0	1.0	275	42	slurry	3550	1050	1745	1983	116	487	587
60	Bangkok, Thailand/dense to very dense sand	57.0	1.50	21.0	1.0	648	42	slurry	33289	5046	10290	23097	555	2047	14865
61	Bangkok, Thailand/dense to very dense sand	57.0	1.50	21.0	1.0	648	42	slurry	33462	8330	12306	18687	916	2580	8842
62	Gulf Coast, Texas/sand	9.1	0.46	19.6	- <sup>l</sup>	179	42	- <sup>n</sup>	1724	928	1360	2693	102	277	1605
63	Arab Gulf, Kuwait/v. dense cemented sand	10.8	0.45	19.6	5.5	160	42	- <sup>n</sup>	1601	1000	1975	3220	110	447	1640
64	Bangkok, Thailand/dense to very dense sand	43.6	1.20	21.0	1.0	498	42	slurry	19301	8718	11209	18267	959	2745	9300
65	Phoenix, Arizona/clayey sand	4.7	0.91	19.6	2.0	66	42	- <sup>n</sup>	4680	2351	5338	8700	259	890	4430
66	Live Oak County, Texas/silty sand	10.1	0.76	19.6	0.0	99	42	dry	3981	1864	5677	9252	205	700	4711
67	Bangkok, Thailand/dense to very dense sand	57.1	1.20	21.0	1.0	649	42	slurry	27132	5338	12010	19509	587	2190	9901
68	Bangkok, Thailand/dense to very dense sand	41.0	1.00	21.0	1.0	469	43	slurry	14551	5004	7384	12035	550	1781	6128
69	Bangkok, Thailand/dense to very dense sand	43.6	1.20	21.0	1.0	498	43	slurry	20433	5693	7206	11745	626	3235	5980
70	Bangkok, Thailand/dense to very dense sand	43.5	1.00	21.0	1.0	497	43	slurry	14217	4448	6405	10701	489	1025	5577
71	Tainan, Taiwan/fine sand	38.2	1.50	18.0	2.6	337	43	slurry	25042	7554	12454	20299	831	3202	10336
72	NR/silty sand	11.0	0.90	20.4	- <sup>l</sup>	224	43	- <sup>n</sup>	7638	3870	9000	14670	426	2136	7470
73	Central Taiwan/silty sand	36.5	1.40	19.6	36.5	716	43	slurry	31973	4113	9638	15710	452	2407	8000
74	Tainan, Taiwan/silty sand	37.0	1.80	19.4	5.2	407	44	casing	43917	5946	14991	24435	654	2892	12442
75	Live Oak County, Texas/silty sand	7.6	0.61	19.6	0.0	75	44	- <sup>n</sup>	3786	1941	6333	8620	214	1060	3553
76	Texas/strongly cemented clayey sand	9.9	0.76	19.6	- <sup>l</sup>	194	44	dry	5753	1001	3114	5186	110	801	2695
77	Bangkok, Thailand/dense to very dense sand	51.0	1.20	21.0	1.0	581	44	slurry	22486	10000	12600	23333	1100	2520	13253
78	Bangkok, Thailand/dense to very dense sand	62.0	1.80	21.0	1.0	704	44	slurry	46693	15667	34000	40000	1723	6880	12800
79	Bangkok, Thailand/dense to very dense sand	30.0	1.00	20.0	1.0	316	44	slurry	11399	5603	12180	17110	616	2436	7366

Pile No.	Location/Soil description	Depth, D(m)	Dia., B(m)	$\gamma_m^a$ (kN/m <sup>3</sup> )	GWT <sup>b</sup> (m)	$\bar{q}^c$ (kN/m <sup>2</sup> )	$\bar{\phi}^d$ (°)	Const. method <sup>m</sup>	$Q_{L1}^e$	$Q_{L2}^f$	$Q_{Chin}^h$	$Q_{L1(ip)}^i$	$Q_{L2(ip)}^j$	$Q_{Chin(ip)}^k$	
80	Bangkok, Thailand/dense to very dense sand	43.0	0.80	21.0	1.0	491	44	slurry	10297	2438	5220	7664	268	1044	3488
81	Bangkok, Thailand/dense to very dense sand	41.0	0.80	21.0	1.0	469	44	slurry	10089	4711	9845	13285	518	1969	5409
82	New Mexico/silty sand	12.2	0.96	19.6	1.2	131	44	- <sup>n</sup>	8179	1500	6840	11987	165	1271	6514
83	Singapore/clayey to silty sand	17.0	1.40	19.6	0.0	167	44	- <sup>n</sup>	21778	14701	21667	35316	1617	4416	17983
84	Arab Gulf, Kuwait/v. dense cemented sand	8.7	0.90	19.6	3.5	120	44	- <sup>n</sup>	6071	3000	8313	13549	330	2155	6899
85	Arab Gulf, Kuwait/v. dense cemented sand	8.5	1.50	19.6	4.5	128	44	- <sup>n</sup>	17399	5600	17667	28797	616	3560	14663
86	Singapore/silty sand	34.0	0.90	19.5	0.0	329	45	casing	11914	3839	6906	9950	422	1847	4425
87	Singapore/silty sand	24.0	0.91	19.5	0.0	233	45	casing	10511	2847	5960	9276	313	1640	4508
88	Singapore/silty sand	35.0	0.80	19.5	0.0	339	45	casing	9740	2847	5516	7832	313	1174	3420
89	Singapore/silty sand	53.0	0.90	19.5	0.0	514	45	casing	14952	3914	9786	13515	431	2034	5687
90	Bangkok, Thailand/dense to very dense sand	24.5	0.90	19.6	0.0	240	45	slurry	10776	6138	11920	16056	675	2135	6520
91	Bangkok, Thailand/dense to very dense sand	53.0	1.00	20.0	1.0	550	45	slurry	15287	5057	11493	16586	556	2299	7392
92	Bangkok, Thailand/dense to very dense sand	55.0	1.00	20.0	1.0	570	45	slurry	15615	3671	7907	12888	404	1837	6562
93	Bangkok, Thailand/dense to very dense sand	55.0	1.00	20.0	1.0	570	45	slurry	15652	5217	12143	17596	574	2429	7882
94	Bangkok, Thailand/dense to very dense sand	55.3	1.50	20.0	1.0	573	45	slurry	35375	6834	15537	25325	752	3637	12895
95	France/medium dense sand	9.8	0.83	17.3	- <sup>l</sup>	170	45	dry	6988	885	1713	4731	97	343	3361
96	San Juan/sand	26.5	0.91	19.6	0.0	260	46	slurry	11074	2771	7869	11409	305	1926	5114
97	Kaohsiung, Taiwan/fine sand	14.0	1.00	19.6	3.4	170	46	- <sup>n</sup>	9364	2611	6032	9832	287	1206	5006
98	Ponce, Puerto Rico/fine sand	15.0	1.52	18.9	5.8	193	46	casing	22938	5355	12454	26430	589	2491	16467
99	Jersey, New Jersey/med to v. dense sand	27.0	0.76	21.0	2.4	326	46	- <sup>n</sup>	7639	3085	7125	10270	339	1425	4570
100	Brownsville, Texas/fine to medium sand	11.6	0.61	17.3	11.6	201	46	- <sup>n</sup>	3963	650	1513	3364	72	303	2154

\*note: except for  $Q_{L1(ip)}$  and  $Q_{Chin(ip)}$  values, other details are from Fang (2007) and Chen *et al.* (2009)

<sup>a</sup>  $\gamma_m$  total unit weight of soil; <sup>b</sup> GWT groundwater table; <sup>c</sup>  $\bar{q}$  vertical effective overburden pressure; <sup>d</sup> average friction angle from triaxial compression, triaxial extension and direct simple shear tests (Kulhawy and Mayne 1990); <sup>e</sup> predicted tip capacity; <sup>f,g,h</sup> interpreted pile capacities from  $L_1$ ,  $L_2$  and Chin methods, respectively; <sup>i,j,k</sup> interpreted tip capacities from  $L_1$ ,  $L_2$  and Chin methods, respectively; <sup>l</sup> groundwater table is below pile tip; <sup>m</sup> construction method; <sup>n</sup> not reported

Table 2 Statistical information for drilled shaft load test data

Statistics <sup>a</sup>	Depth, $D$ (m)	Diameter, $B$ (m)	D/B	$\bar{\phi}_{avg}$ <sup>b</sup> (°)	$Q_{L2}$ <sup>c</sup> (kN)	$Q_{L2(tip)}$ <sup>d</sup> (kN)
$n$	100	100	100	100	100	100
Range	5-69	0.2-2.0	5.1-62.5	31-46	180-35821	36-6800
Mean	28.4	1.0	28.1	39.8	7853	1530
SD	18.1	0.4	14.4	4.2	6875	1270
COV	0.64	0.39	0.51	0.11	0.88	0.83

<sup>a</sup>  $n$  = number of data, SD = standard deviation, COV = coefficient of variation

<sup>b</sup> average friction angle from triaxial compression, triaxial extension, and direct simple shear tests

<sup>c</sup> interpreted pile capacity by  $L_2$  method

<sup>d</sup> interpreted tip capacity by  $L_2$  method

(failure threshold). The capacity by Chin is extrapolated by dividing each settlement with its corresponding load, and plotting the resulting value against the settlement. An approximate linear relationship can be observed. The inverse slope of this line is the interpreted capacity by Chin. Chen *et al.* (2008), Chen and Fang (2009), and Chen and Chu (2012) suggested that the interpretation limits for engineering design, including the lower limit (allowable load stage), the middle (design load stage), and the upper limit (limit failure load stage) as shown in Fig. 2 can be represented by  $L_1$ ,  $L_2$ , and Chin, respectively.

The measured tip resistance ( $Q_{tcm}$ ) can be proportioned from the total interpreted compression capacity using the load-distribution curve along the shaft length. However, some load tests are not instrumented with strain gages. Previously, Chen and Kulhawy (1994) and Fang (2007) utilized field load test data to assess the distribution ratio of the tip and side capacities. Results from these studies show that the tip capacity from  $L_1$  and  $L_2$  methods can be proportioned as 11% and 20% of the total capacity, respectively. Alternatively, these results are adopted to infer the  $Q_{tcm}$  in cases where the load test report did not present the load distribution curve. The interpreted capacity by Chin (1970) basically occurs at relatively large displacement, in which the side resistance is essentially completed. Chen and Kulhawy (1994) and Chen *et al.* (2011) reviewed the side resistance of drilled shafts using a large number of field test data and demonstrated that the predicted and measured side resistances are relatively comparable and consistent. Therefore, the tip bearing capacity by Chin is defined as the total interpreted capacity minus the predicted side resistance. The tip capacities from  $L_1$ ,  $L_2$ , and Chin are also listed in Table 1 as  $Q_{L1(tip)}$ ,  $Q_{L2(tip)}$ , and  $Q_{Chin(tip)}$ , respectively.

For convenience, the ranges of shaft geometry, soil strength data, compression capacity, and coefficient of variation (COV), which is the standard deviation (SD) divided by the mean value, are summarized in Table 2. The ranges of geometry, soil friction angle, and tip capacity are broad. Therefore, these load test data can be considered as representative for the present study.

### 3. Description of analysis model

The capacity of a drilled shaft in axial compression is the sum of the shaft tip capacity and side resistance. Tip resistance is provided by the bearing capacity of the soil beneath the tip and can be assessed by a commonly used bearing capacity theory. The ultimate bearing capacity ( $q_{ult}$ ) is

evaluated and multiplied by pile area ( $A_{tip}$ ) to predict the tip capacity ( $Q_{tcp}$ ), as follows

$$Q_{tcp} = q_{ult} \times A_{tip} \quad (1)$$

The ultimate bearing capacity equation has been modified by many researchers. A few of these modifications were presented by Hansen (1970), Vesic (1975), Kulhawy (1991), and Chen and Kulhawy (1994). In drilled shaft design, one of the frequently used bearing capacity equation for cohesionless soils is

$$q_{ult} = \bar{q} N_q \zeta_{qs} \zeta_{qd} \zeta_{qr} + 0.3 \bar{\gamma} B N_\gamma \zeta_{\gamma r} \quad (2)$$

where  $\bar{q}$  is the vertical effective overburden pressure.  $N_q$  and  $N_\gamma$  are bearing capacity and overburden pressure factors, respectively.  $\zeta_{qs}$ ,  $\zeta_{qd}$ , and  $\zeta_{qr}$  are the modifiers of  $N_q$  for foundation shape (s), depth (d), and soil rigidity (r), respectively.  $\gamma$  is the effective unit weight of soil.  $B$  is the shaft diameter, and  $\zeta_{\gamma r}$  is the modifier of  $N_\gamma$  for soil rigidity. The detailed calculation of the factors and modifiers can be found in the literature (Kulhawy 1991, Chen and Kulhawy 1994, Das 2010). These factors are basically related to the soil effective friction angle ( $\bar{\phi}$ ) beneath the shaft tip. Based on a number of analyses in pile foundations that utilized this equation, the second term ( $0.3 \bar{\gamma} B N_\gamma \zeta_{\gamma r}$ ) accounts for a negligibly small proportion of the overall capacity.

#### 4. Research methods

The ultimate bearing capacity equation [Eq. (2)] is improved to facilitate a more reasonable estimation of drilled shaft tip capacity. The factors and modifiers in the equation are assessed in detail. However, as previously mentioned, the second term of the equation provides very small proportion of the tip capacity compared with the first term. Therefore, the assessment is focused on the parameter  $\bar{q}$  and factors  $N_q$ ,  $\zeta_{qs}$ ,  $\zeta_{qd}$ , and  $\zeta_{qr}$ . The statistics for these coefficients based on the originally predicted tip resistance (Chen *et al.* 2009) for the 100 drilled shaft load tests are demonstrated in Table 3 to compare their variability. From the statistics, the parameter  $\bar{q}$  and factors  $N_q$  and  $\zeta_{qr}$  demonstrate considerably large coefficients of variation of 0.61, 0.54, and 0.51, respectively. The results are consistent with those in the previous studies, where these factors exhibit larger range of values among others. Hence, these factors are considered for the improvement analysis of the bearing capacity equation.

To rationally represent the measured tip capacity and for practical engineering applications, loading stages  $L_1$ ,  $L_2$ , and Chin are adopted in the improvement. These limits possess different factors to reflect various mobilized displacement states.

Based on previous analysis (Chen *et al.* 2009), the large variation is very explicit in shafts with longer lengths. This manifestation reveals that the effective overburden pressure beneath the shaft tip can greatly affect the behavior of the shaft. Therefore, varying effective depths, such as 10B, 15B, 20B, and 30B are considered to explore the effect of shaft depth and be the basis for the improvement of the factors. The calculation of the parameter  $\bar{q}$  is limited to the effective depth in cases where the shaft length exceeds the effective depth. The  $N_q \zeta_{qr}$  values are back-calculated for different loading stages at different effective depths using the measured tip capacity ( $Q_{tcm}$ ) and Eq. (2) for the 100 field load tests. The  $N_q \zeta_{qr}$  value is the product of any values of  $N_q$  and  $\zeta_{qr}$ . To obtain possible combinations of these two terms, Fortran program is used. Boundary conditions which are based on the original range of  $\zeta_{qr}$  (Fang 2007) are imposed for Fortran to generate random

Table 3 Statistical comparison of bearing capacity factors and modifiers

Statistics <sup>a</sup>	$N_q$	$\zeta_{qs}$	$\zeta_{qd}$	$\zeta_{qr}$	$\bar{q}$ (kN/m <sup>2</sup> )
$n$	100	100	100	100	100
Min.	21.63	1.61	1.24	0.09	37.18
Max.	164.07	2.04	1.42	0.94	766.52
Mean	75.37	1.84	1.33	0.30	323.87
SD	40.93	0.12	0.05	0.15	199.08
COV	<b>0.54</b>	0.07	0.04	<b>0.51</b>	<b>0.61</b>

<sup>a</sup>  $n$  = number of data, SD = standard deviation, COV = coefficient of variation

combinations of  $N_q$  and  $\zeta_{qr}$ . To obtain the most acceptable values of  $N_q$  and  $\zeta_{qr}$  from the many possible combinations generated by Fortran, the MATLAB program is used. MATLAB is adopted because of its simplicity in designing the programming syntax. Previous studies (Hansen 1970, Vesic 1975, Kulhawy 1991) verified that  $N_q$  and  $\zeta_{qr}$  have consistent relationship with  $\bar{\phi}$ , in which  $N_q$  increases and  $\zeta_{qr}$  decreases as  $\bar{\phi}$  increases. The physical meaning of this principle is maintained and adopted as the basis for selecting  $N_q$  and  $\zeta_{qr}$  combinations.

All of the combinations of  $N_q$  and  $\zeta_{qr}$  are run in MATLAB program to select the combinations that maintain the relation of  $\bar{\phi}$  with  $N_q$  and  $\zeta_{qr}$ . Subsequently, the MATLAB selected values of  $N_q$  and  $\zeta_{qr}$  are plotted against  $\bar{\phi}$ . The regression curve and statistics of the data points are obtained and evaluated. The most acceptable set of data combination is defined by the highest sum of the coefficient of determination ( $r^2$ ) of these two factors.

## 5. Analysis results

The comparison of analysis results are presented in Tables 4 to 6 for  $L_1$ ,  $L_2$ , and Chin methods, respectively. The regression analyses [standard deviation (SD) and coefficient of determination ( $r^2$ )] for  $N_q$  and  $\zeta_{qr}$  and for the improved relationship ( $\chi$ ) of predicted and measured tip capacities for the different shaft depths are likewise noted in Tables 4 to 6. Although the differences are small for all interpretation criteria, the sum of  $r^2$  values of  $N_q$  and  $\zeta_{qr}$  is a maximum at a shaft depth

Table 4 Comparison of analysis results for different effective depths using  $L_1$  method

Factor	10B		15B		20B		30B					
	SD	$r^2$	SD	$r^2$	SD	$r^2$	SD	$r^2$				
$N_q$	0.33	0.84	0.32	0.84	0.33	0.79	0.27	0.66				
$\zeta_{qr}$	0.29	0.82	0.28	0.83	0.28	0.76	0.29	0.68				
$Q_{tcm} = \chi Q_{tcp}$	SD (kN)	$r^2$	$\chi$									
	211	0.82	0.98	210	0.83	0.99	238	0.81	1.01	303	0.71	1.00

\*Note: SD: standard deviation ;  $r^2$ : coefficient of determination

Table 5 Comparison of analysis results for different effective depths using  $L_2$  method

Factor \ Effective depth	10B		15B			20B			30B			
	SD	$r^2$	SD	$r^2$	$\chi$	SD	$r^2$	$\chi$	SD	$r^2$	$\chi$	
$N_q$	0.36	0.88	0.35	0.88		0.42	0.84		0.40	0.82		
$\zeta_{qr}$	0.31	0.77	0.31	0.78		0.39	0.72		0.33	0.73		
$Q_{tcm} = \chi Q_{tcp}$	SD (kN)	$r^2$	$\chi$	SD (kN)	$r^2$	$\chi$	SD (kN)	$r^2$	$\chi$	SD (kN)	$r^2$	$\chi$
	615	0.87	0.99	610	0.87	1.00	644	0.86	0.98	723	0.82	1.03

\*Note: SD: standard deviation ;  $r^2$ : coefficient of determination

Table 6 Comparison of analysis results for different effective depths using Chin method

Factor \ Effective depth	10B		15B			20B			30B			
	SD	$r^2$	SD	$r^2$	$\chi$	SD	$r^2$	$\chi$	SD	$r^2$	$\chi$	
$N_q$	0.36	0.83	0.34	0.83		0.32	0.82		0.31	0.61		
$\zeta_{qr}$	0.31	0.76	0.31	0.77		0.31	0.73		0.30	0.71		
$Q_{tcm} = \chi Q_{tcp}$	SD (kN)	$r^2$	$\chi$	SD (kN)	$r^2$	$\chi$	SD (kN)	$r^2$	$\chi$	SD (kN)	$r^2$	$\chi$
	2298	0.88	0.98	2280	0.88	0.99	2504	0.86	0.99	3484	0.72	1.05

\*Note: SD SD: standard deviation ;  $r^2$ : coefficient of determination

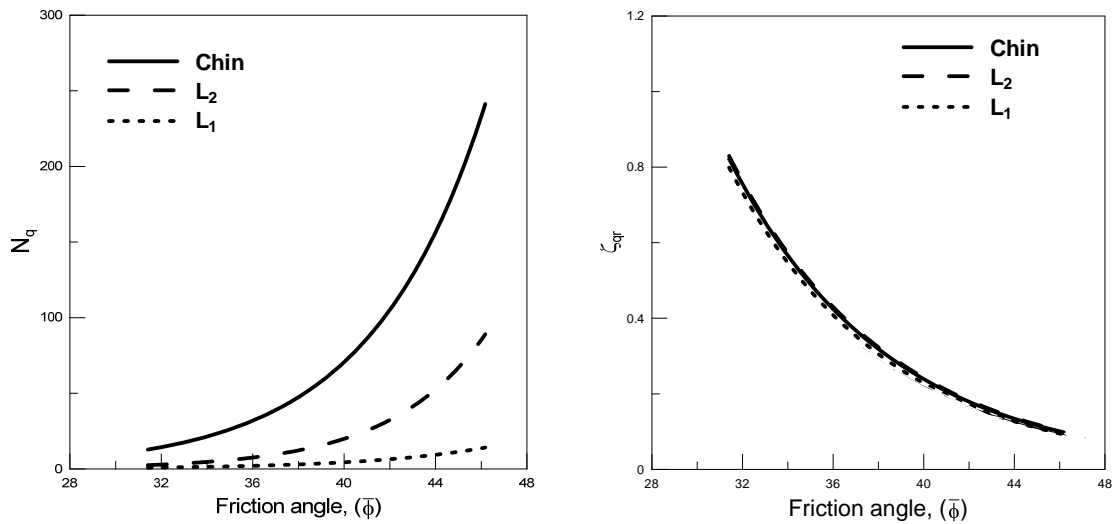


Fig. 3 Relation of  $N_q$  and  $\zeta_{qr}$  factors with  $\bar{\phi}$  for drilled shafts in cohesionless soils

of 15B, indicating as the most acceptable combination. The mean of the measured values is also very close to the predicted values (i.e.,  $\chi \approx 1$ ) at a depth of 15B. Therefore, the effective depth for drilled shaft in cohesionless soils can be best limited to 15B for the tip capacity analysis.

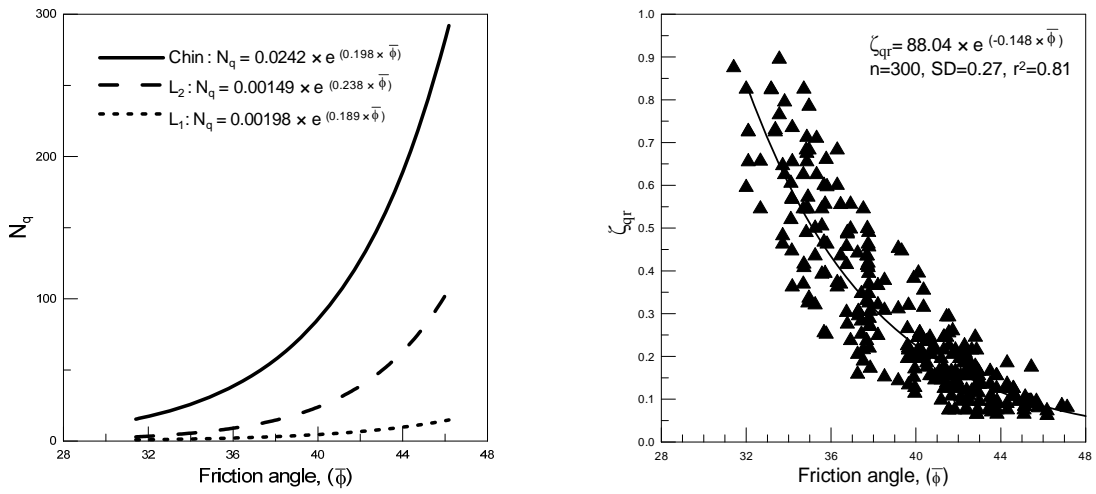
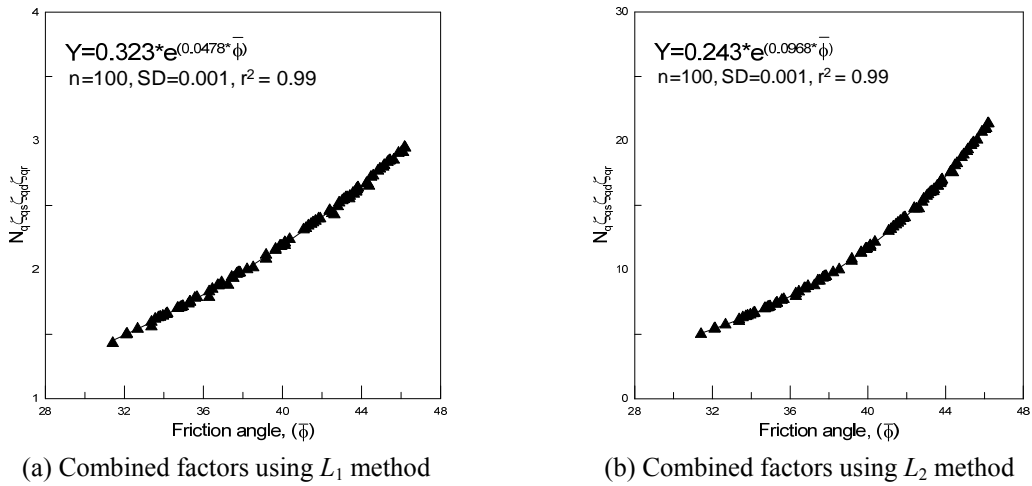
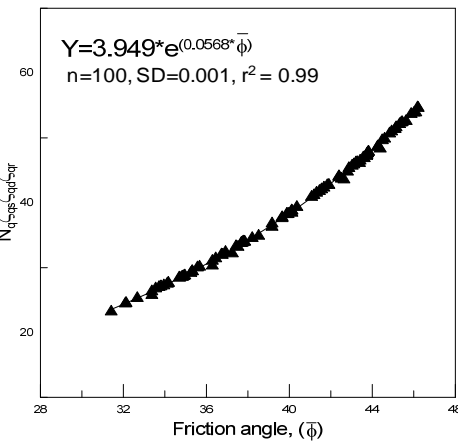


Fig. 4 Proposed equation of  $N_q$  and  $\zeta_{qr}$  factors for drilled shafts in cohesionless soils



(a) Combined factors using  $L_1$  method

(b) Combined factors using  $L_2$  method



(c) Combined factors using Chin method

Fig. 5 Simplified factor ( $\bar{N}_q$ ) for each interpretation criterion

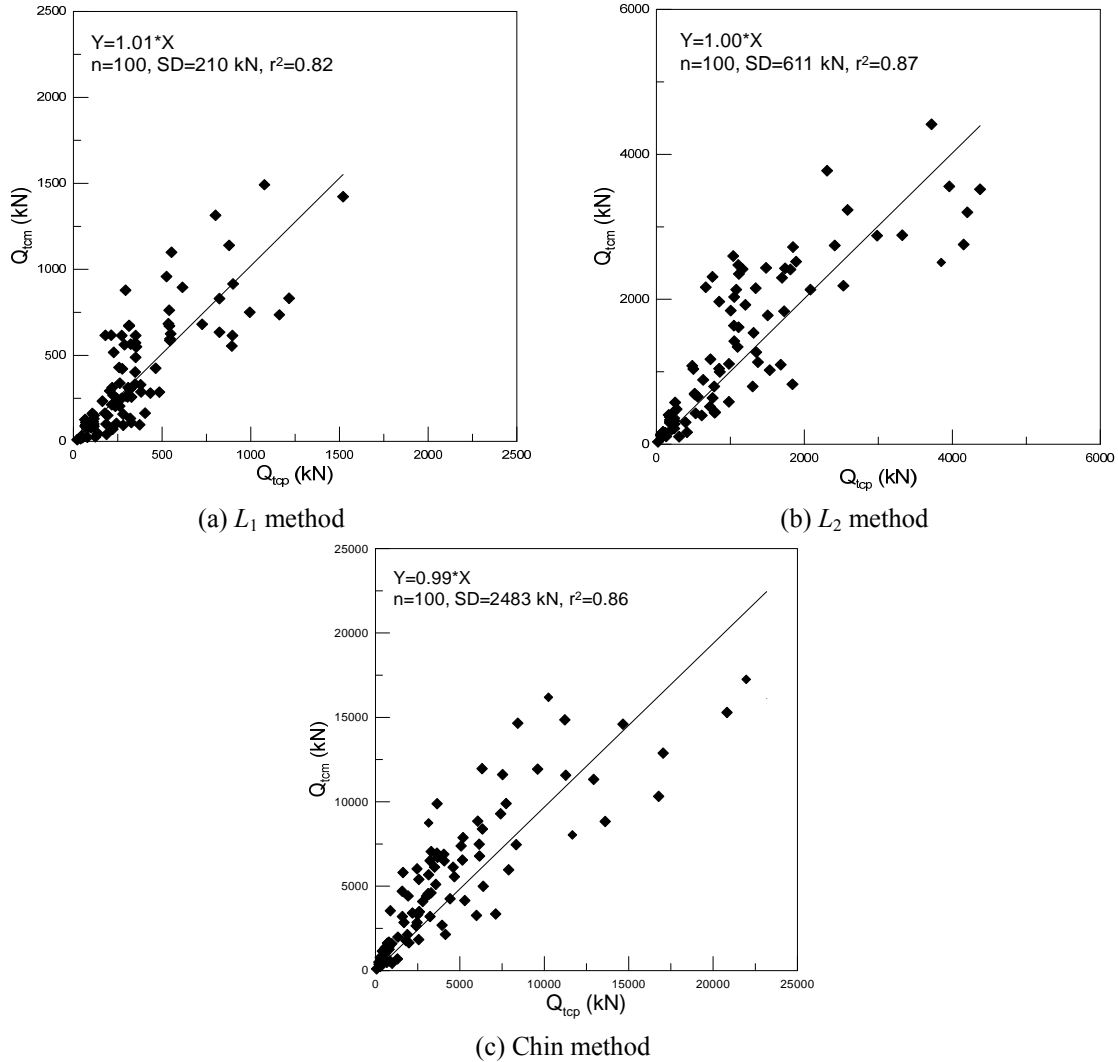


Fig. 6 Comparisons of  $Q_{tcm}$  and  $Q_{tcp}$  after improvement

The regression curves for the 100 data points under effective depth of 15B are illustrated in Fig. 3. For clarity of the curves, the data points are omitted in the figure. The correlations between  $N_q$  and  $\bar{\phi}$ , as well as that of  $\zeta_{qr}$  and  $\bar{\phi}$ , for the different interpretation criteria are compared. The  $N_q$  and  $\bar{\phi}$  variations from the largest interpretation criterion (Chin method), to the  $L_2$  method, and to the smallest criterion ( $L_1$ ) is consistent with the theoretical results. The  $\zeta_{qr}$  and  $\bar{\phi}$  variations relative to the interpretation criteria is very small and shows a consistent trend. Hence, the results from Chin,  $L_2$ , and  $L_1$  methods for the correlation between  $\zeta_{qr}$  and  $\bar{\phi}$  are merged for convenient engineering design application and set as the basis to establish a new correlation as shown in Fig. 4. The data set provides a simplified equation for the evaluation of  $\zeta_{qr}$ . Based on the combined  $\zeta_{qr}$  and  $\bar{\phi}$  correlation, new regression curves for  $N_q$  and  $\bar{\phi}$  are obtained and shown in Fig. 4.

Given that the factors  $N_q$ ,  $\zeta_{qs}$ ,  $\zeta_{qd}$ , and  $\zeta_{qr}$  in the first term of the bearing capacity equation are all related to the soil effective friction angle, the relation of the combination of these factors and friction angle is noteworthy. The correlation between  $\bar{N}_q$  (comprising the factors  $N_q$ ,  $\zeta_{qs}$ ,  $\zeta_{qd}$ , and  $\zeta_{qr}$ ) and  $\bar{\phi}$  under the different interpretation criteria is demonstrated in Fig. 5. The analysis results are also listed in Fig. 5. The equations for these correlations are established for tip bearing capacity evaluation. The statistics are evidently consistent, indicating reasonable results. Hence, these relationships can be applied for drilled shaft analysis and design.

The predicted ( $Q_{tip}$ ) and measured tip capacities ( $Q_{tcm}$ ) after enhancements are noted in Fig. 6 to assess the effect of the improvements. On the average, the predicted tip capacities using the improved analysis model are fairly consistent with the measured capacities. Comparison of Figs. 1 and 6 clearly indicates that the predicted results are greatly enhanced. The statistical results in Fig. 6 also indicate an improved  $r^2$ . Therefore, the improved equations derived from the present study can reasonably estimate the drilled shaft tip bearing capacity in cohesionless soils. The second term of the bearing capacity equation ( $0.3\bar{\gamma}BN_\gamma\zeta_{\gamma r}$ ) has considerable impact when  $L_1$  method is used, and thus, should not be neglected in the analysis. Evaluation of the  $L_2$  and Chin methods indicates that the effect of this term is negligibly small. Although the results are conservative to a certain extent, the simplified equation can provide quick estimates.

## 6. Design recommendations

Based on the evaluation of tip bearing capacity of drilled shafts in cohesionless soils, the following conditions are recommended for practical use in engineering analysis and design:

- The effective overburden pressure can be limited to a shaft depth of 15B.
- A single equation for the improved modifier  $\zeta_{qr}$  can be adopted for the interpretation criteria as

$$\zeta_{qr} = 88.04 \times e^{(-0.148 \times \bar{\phi})} \quad (3)$$

- The factor  $N_q$  for the interpretation criteria can be calculated as follows

$$L_1 \text{ method : } N_q = 0.00198 \times e^{(0.189 \times \bar{\phi})} \quad (4)$$

$$L_2 \text{ method : } N_q = 0.00149 \times e^{(0.238 \times \bar{\phi})} \quad (5)$$

$$\text{Chin method : } N_q = 0.0242 \times e^{(0.198 \times \bar{\phi})} \quad (6)$$

- From the combination of the improved factors, the simplified tip bearing capacity equations are as follows

$$L_1 \text{ method : } q_{ult} = \bar{q} \times 0.323 \times e^{(0.0478 \times \bar{\phi})} + 0.3\bar{\gamma}BN_\gamma\zeta_{\gamma r} \quad (7)$$

$$L_2 \text{ method : } q_{ult} = \bar{q} \times 0.243 \times e^{(0.0968 \times \bar{\phi})} + 0.3\bar{\gamma}BN_\gamma\zeta_{\gamma r} \quad (8)$$

$$\text{Chin method : } q_{ult} = \bar{q} \times 3.949 \times e^{(0.0568 \times \bar{\phi})} + 0.3\bar{\gamma}BN_\gamma\zeta_{\gamma r} \quad (9)$$

- The term  $0.3\bar{\gamma}BN_\gamma\zeta_{\gamma r}$  is suggested to be retained when the  $L_1$  method is applied because of its considerable impact. For  $L_2$  and Chin methods, however, the term is negligibly small and

may be disregarded. The result is somehow conservative but can facilitate faster calculations.

## 7. Conclusions

The present study employed 100 axial compression field load tests to improve an analysis model for tip bearing capacity. Previous studies have shown that the model greatly overestimated the drilled shaft tip capacity in cohesionless soils. The factors in the analysis model that revealed greater variations were carefully evaluated from the back analysis of field load tests to deduce the best results. Thus, new correlations of the factors and simplified equations that reasonably predicted the tip capacity were derived. Specific design recommendations based on the analyses results were suggested for an improved model for the calculation of the tip bearing capacity of drilled shafts in cohesionless soils.

## Acknowledgements

This study was supported by the National Science Council, Taiwan, under contract number: NSC 100-2221-E-033-073-MY3.

## References

- Cai, G., Liu, S. and Puppala, A.J. (2012), "Reliability assessment of CPTU-based pile capacity predictions in soft clay deposits", *Eng. Geo.*, **141-142**, 84-91.
- Cai, G., Liu, S., Tong, L. and Du, G. (2009), "Assessment of direct CPT and CPTU methods for predicting the ultimate bearing capacity of single piles", *Eng. Geo.*, **104**(3-4), 211-222.
- Chen, C.H. (2010), "Evaluation of compression behavior for digging construction pre-bored PC piles in drained soils", *Master Thesis*, Department of Civil Engineering, Chung Yuan Christian University, Chung Li, Taiwan.
- Chen, Y.J. and Chu, T.H. (2012), "Evaluation of uplift interpretation criteria for drilled shafts in gravelly soils", *Can. Geotech. J.*, **49**(1), 70-77.
- Chen, Y.J. and Fang, Y.C. (2009), "Critical evaluation of compression interpretation criteria for drilled shafts", *J. Geotech. Geoenviron. Eng.*, **135**(8), 1056-1069.
- Chen, Y.J. and Kulhawy, F.H. (1994), "Case history evaluation of drilled shaft behavior", *Rpt TR-104601*, Electric Power Research Institute, Palo Alto.
- Chen, Y.J., Chang, H.W. and Kulhawy, F.H. (2008), "Evaluation of uplift interpretation criteria for drilled shaft capacity", *J. Geotech. Geoenviron. Eng.*, **134**(10), 1459-1468.
- Chen, Y.J., Fang, Y.C. and Chu, T.H. (2009), "Evaluation of compression tip capacity for drilled shafts", *Proceedings of International Foundation Congress and Equipment Expo*, Orlando, Florida, March.
- Chen, Y.J., Lin, S.S., Chang, H.W. and Marcos, M.C. (2011), "Evaluation of side resistance capacity for drilled shafts", *J. Marine Sci. Tech.*, **19**(2), 210-221.
- Chin, F.K. (1970), "Estimation of the ultimate load of piles not carried to failure", *Proceedings of 2<sup>nd</sup> Southeast Asian Conference on Soil Engineering*, Singapore, June.
- Ching, J. and Chen, J.R. (2010), "Predicting displacement of augered cast-in-place piles based on load test database", *Struct. Saf.*, **32**(6), 372-383.
- Chu, T.H. (2009), "Evaluation of interpretation criteria and capacity for drilled shafts in gravelly soils under axial and lateral loading", *Master Thesis*, Department of Civil Engineering, Chung Yuan Christian

- University, Chung Li, Taiwan.
- Das, B.M. (2010), *Principles of Foundation Engineering*, (7th Edition), Cengage Learning.
- Department of the Navy, Naval Facilities Engineering Command (NAVFAC) (1982), *Foundation and Earth Structure*, Design Manual 7.2”.
- Fang, Y.C. (2007), “Evaluation of tip resistance and compression interpretation criteria for drilled shafts”, *Master Thesis*, Department of Civil Engineering, Chung Yuan Christian University, Chung Li, Taiwan.
- Hansen, J.B. (1970), “A revised and extended formula for bearing capacity”, Bull. 28, Danish Geotechnical Institute, Copenhagen, 5-11.
- Hirany, A. and Kulhawy, F.H. (1988), “Conduct and interpretation of load tests on drilled shaft foundations”, Detailed Guidelines, *Rpt EL-5915(1)*, Electric Power Research Institute, Palo Alto.
- Hirany, A. and Kulhawy, F.H. (2002), “On the interpretation of drilled foundation load test results”, *Proceedings of International Deep Foundations Congress*, Orlando, Florida, February.
- Kulhawy, F.H. (1991), “Drilled Shaft Foundations”, Chapter 14: in *Foundation Engineering Handbook* (2nd Edition), Van Nostrand Reinhold, N.Y.
- Kulhawy, F.H. and Mayne, P.W. (1990), “Manual on estimating soil properties for foundation design”, *Report EL-6800*, EPRI, Palo Alto.
- Kulhawy, F.H., Trautmann, H.C., Beech, J.F., O'Rourke, T.D., McGuire, W., Wood, W.A. and Capano, C. (1983), “Transmission line structure foundations for uplift-compression loading”, *Rpt EL-2870*, EPRI, Palo Alto.
- Marcos, M.C., Chen, C.H. and Chen, Y.J. (2011), “Evaluation of axial capacity of pre-bored PC piles in drained soils”, *J. Adv. Eng.*, **6**(4), 321-326.
- Schneider, J., Xu, X. and Lehane, B.M. (2008), “Database assessment of CPT-based design methods for axial capacity of driven piles in siliceous sands”, *J. Geotech. Geoenviron. Eng.*, **134**(9), 1227-1244.
- Vesic, A.S. (1963), “Bearing capacity of deep foundation in sand”, *Highway Research Board Record*, No. 39, 112-153.
- Vesic, A.S. (1975), “Bearing capacity of shallow foundation”, Chapter 3: in *Foundation Engineering Handbook*, Van Nostrand Reinhold, N.Y.
- Zhang, L.M., Shek, L.M.P., Pang, H.W. and Pang C.F. (2006), “Knowledge-based design and construction of driven piles”, *Proceedings of the Institution of Civil Engineers: Geotech. Eng.*, **159**(3), 177-185.